THE ASTROPHYSICAL JOURNAL, 335:290–294, 1988 December 1

DETECTION OF CIRCULAR POLARIZATION IN R MONOCEROTIS AND NGC 2261: IMPLICATIONS FOR THE POLARIZATION MECHANISM

FRANÇOIS MÉNARD, PIERRE BASTIEN, AND CARMELLE ROBERT
Observatoire du Mont Mégantic and Département de Physique, Université de Montréal
Received 1988 March 25; accepted 1988 May 28

ABSTRACT

We report the detection of circular polarization from R Mon and also at positions in its nebulosity 5″–7″ from the star. We made a null detection at one of five positions observed in the NGC 2261 reflection nebula. Implications of these observations for the mechanism responsible for the linear and circular polarization are discussed. We conclude that multiple scattering in a flattened distribution is the most likely mechanism in this object and possibly in many other ones. This interpretation means that linear polarization maps provide *direct* evidence for circumstellar disks around young stellar objects.

Subject headings: nebulae: individual (NGC 2261) — nebulae: reflection — polarization — stars: circumstellar shells — stars: individual (R Mon)

I. INTRODUCTION

At a distance of 800 pc (Walker 1956) R Mon has an inferred luminosity of about 1400 $L_\odot$ (Cohen *et al.* 1984). This high-energy output makes it probably the most massive young stellar object (YSO) to show a highly collimated optical jet (Brugel, Mundt, and Bührke 1984). Moreover R Mon and its associated nebulosity NGC 2261 has been known for some time to exhibit high levels of variable linear polarization in the 11%–16% range for R Mon (Hall 1965; Zellner 1970; Garrison and Anderson 1978; Jones and Dyck 1978; Vrba, Schmidt, and Hintzen 1979) and 20%–30% range for NGC 2261 (Hall 1964, 1965). More recently a southern extension to NGC 2261 was discovered by Walsh and Malin (1985) and it is also highly polarized at 30%–40% (Warren-Smith, Draper, and Scarrott 1987).

Generally, it is admitted that NGC 2261 and its southern extension are both reflection nebulae, the illuminating source being R Mon. Evidence for this comes from the centrosymmetric pattern of the measured linear polarization vectors (Gething *et al.* 1982; Aspin, McLean, and Coyne 1985; Warren-Smith, Draper, and Scarrott 1987), all the vectors lying perpendicular to the radial direction to R Mon. This is certainly the case in NGC 2261 at distances greater than 20″ from R Mon. Such a centrosymmetric pattern is typical of reflection nebulae where single scattering is responsible for the polarization since the polarization vectors are usually perpendicular to the scattering plane.

However, departure from this single-scattering pattern is clearly seen in a band close to and including R Mon itself. In this band the polarization vectors are roughly perpendicular to the symmetry axis of the bipolar nebula. The presence of such a region of aligned polarization vectors is common in YSOs associated with reflection nebulosity (Bastien 1988*a*). Until recently, these patterns of aligned polarization vectors were usually interpreted as due to dichroic extinction by elongated grains aligned by a toroidal magnetic field, this toroidal field being the remnant of the gravitational collapse of a molecular cloud with a frozen-in magnetic field (e.g., Mestel and Paris 1984). It is not clear, however, that the bipolar nebula formed this way would have a toroidal field. In fact competing scenarios where the magnetic field is more perpendicular to the disk were proposed by Pudritz and Norman (1983) and Pudritz and Silk (1987). These latter authors mention that ambipolar diffusion would prevent the toroidal component from becoming more important than the perpendicular component.

However, Bastien and Ménard (1988, hereafter BM) have proposed recently an alternative way to produce patterns of aligned polarization vectors in YSOs. Their mechanism makes no assumption whatsoever about the grain size and shape and requires no magnetic field. The only requirements concern the geometry of the bipolar nebula itself. The bipolar lobes have to be optically thin while the equatorial disk should be optically thick. We note here that this is precisely the geometry generally adopted for the R Mon/NGC 2261 complex. Single scattering in the optically thin lobes naturally gives a centrosymmetric pattern while the large optical depth in the equatorial disk ensures multiple scattering. This multiply scattered light is, according to the BM model, the key factor to produce bands of aligned polarization vectors in YSOs. Indeed, consideration of double scattering only was sufficient to explain all (but may be one) polarization maps published so far. Similar results were proposed by Notni (1983), but he assumed that the light coming from the star was already polarized (by aligned grains closer to it!); his results nevertheless provide additional support for the model proposed by BM.

A typical circular polarization pattern is predicted from the BM model (Bastien 1988*b*). Notni (1983), with his additional assumptions, predicted a similar pattern, and also Shafter and Jura (1980) who computed circular polarization from Mie scattering in a circumstellar shell of light already linearly polarized. According to this characteristic pattern, the circular polarization has a different sign in each adjacent quadrant. The quadrants are defined by the projection of the outflow axis on the plane of the sky and a perpendicular to it passing through the star.

Circular polarization observations of R Mon/NGC 2261 were carried out to verify the prediction of circular polarization from the BM model. After presenting the observations we show that multiple scattering is required and that aligned grains are not suitable to explain the data.

II. OBSERVATIONS

The observations were made on 1988 January 22, 23, and 27 with the 1.6 m Ritchey-Chrétien telescope of the Mont Mégantic Observatory in Québec, Canada. We used a two-channel photoelectric polarimeter at the f/15 Cassegrain focus. The incident light is analyzed by a Pockels cell modulator followed by a Wollaston prism. The system efficiency was checked with a right circular polarizer and found to be 93%–94% on every night. A small instrumental circular polarization was determined, and later subtracted from the data, by measuring standard linearly unpolarized stars. All the measurements were made with the same Schott RG 645 filter which, coupled with the RCA C31034A photomultipliers, defines a 2450 Å wide bandpass centered at 7675 Å. The observing procedure was the same as that followed by Nadeau and Bastien (1986).

On January 22 and 23 linear polarization measurements of R Mon were taken prior to switching to the circular polarization mode. Circular polarization measurements were taken on the star itself and also at five different positions as shown in Figure 1. This contour map was produced from a 1600 s CCD *R* frame taken at the Mont Mégantic Observatory.

The linear polarization data are presented in Table 1. The columns give respectively the aperture size used, ϕ_d, the polarization, P, its associated error from photon counting statistics, $\sigma(P)$, the equatorial position angle, θ, measured eastward of north, its error, $\sigma(\theta)$, and also the Julian date, JD, corresponding to the middle of each observation.

TABLE 1

LINEAR POLARIZATION DATA FOR R MONOCEROTIS

ϕ_d (″)	P (%)	$\sigma(P)$ (%)	θ (°)	$\sigma(\theta)$ (°)	JD −2,447,180.0
3.9.....	12.74	0.08	97.8	1.0	0.668
8.3.....	13.34	0.05	90.6	1.0	3.480
3.9.....	12.26	0.06	92.2	1.0	3.493
3.9.....	12.35	0.06	88.7	1.0	4.489

The circular polarization data are presented in Table 2 where the usual astronomical convention has been followed, i.e., right circular polarization has a positive sign. The columns show respectively the position of the measurements (cf. Fig. 1), the aperture size used, the circular polarization, V/I, in units of 10^{-4}, the associated error, $\sigma(V/I)$, in the same units, then n, the number of 600 s integrations that were taken and finally the circular polarization divided by its error, S/N.

As can be seen in Table 2, there is strong circular polarization from R. Mon and its immediate vicinity. Furthermore, the sign of the circular polarization is different for the star itself

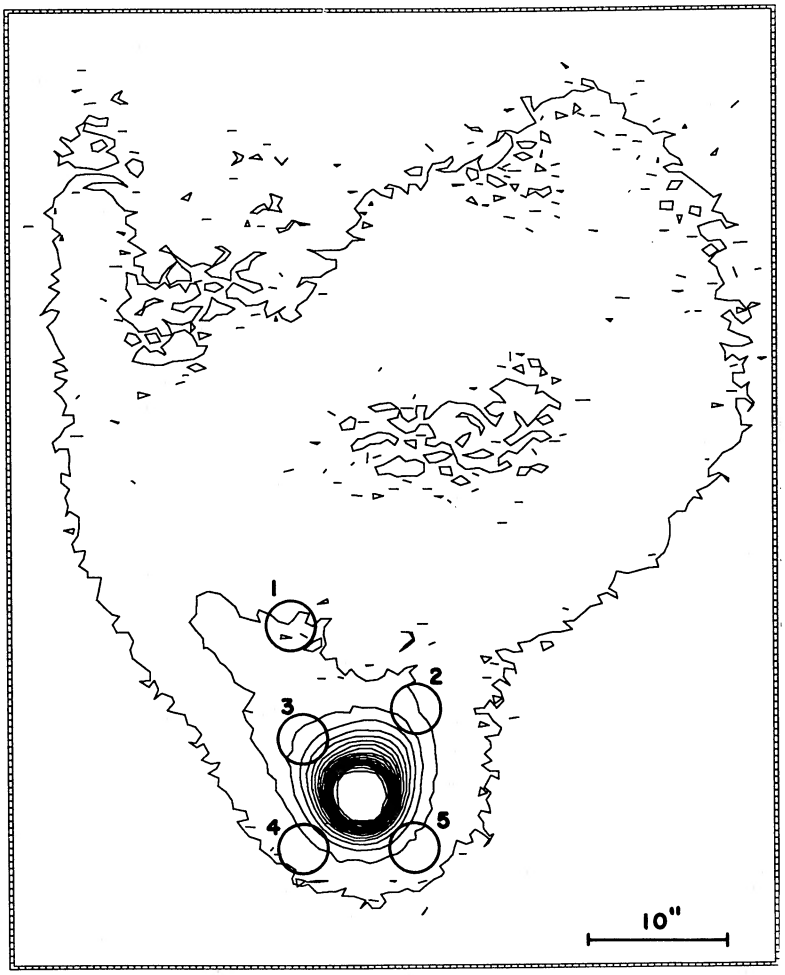

FIG. 1.—A CCD *R* band contour map of R Mon/NGC 2261 which shows the positions (cf. Table 2) where circular polarization measurements were taken. The size of the circles represents the actual diaphragm size. North is up and East to the left on this picture.

TABLE 2

CIRCULAR POLARIZATION DATA FOR R MONOCEROTIS AND NGC 2261[a]

Position	ϕ_d (″)	V/I 10^{-4}	$\sigma(V/I)$ 10^{-4}	n	S/N
R Mon	3.9	10.9	2.2	2	4.9
R Mon	8.3	−13.5	1.3	6	10.1
1	3.9	−1.2	4.5	6	0.3
2	3.9	−16.8	6.3	4	2.7
3	3.9	−20.4	6.7	3	3.1
4	3.9	−37.2	5.6	4	6.7
5	3.9	−11.1	6.2	4	1.8

[a] Values of linear polarization at the same positions than those for which circular polarization is given here can be found from the recently published linear polarization map by Warren-Smith, Draper, and Scarrott (1987).

(as far as it can be resolved by a 3″.9 diaphragm) and for regions about 5″–7″ around it. The circular polarization is particularly strong to the south-east and north-east of R Mon. Farther away from the star, at position 1, the circular polarization is consistent with zero.

III. DISCUSSION

a) A Circumstellar Origin

We can reject instrumental effects as an explanation for our detections since each measurement was taken at two perpendicular positions of the polarimeter in order to eliminate possible conversion of linear to circular polarization. In the Appendix, we show that expected cross-talk effects are significantly smaller than what we measured. A second argument comes from the data: we would not expect to get essentially zero circular polarization at position 1, where the linear polarization is strongest, if instrumental effects were not eliminated properly.

We can discard an interstellar (IS) origin for the detected circular polarization for two reasons.

1. The circular polarization varies by more than an order of magnitude across the nebula; it is zero at position 1 and even changes sign near R Mon. Circular polarization can be produced in the IS medium by two clouds of aligned dust grains with different alignment directions along the line of sight (Kemp and Wolstencroft 1972; Martin 1974), or by transformation of intrinsic linear polarization into circular polarization (e.g., Nadeau and Bastien 1986). However, the former can be rejected since the large range of variations across the nebula would require that the IS medium be inhomogeneous on a few arcsecond scale, which is very unlikely. The latter is rejected because position 1 is associated with the highest linear polarization at approximately the same position angle than positions 3 and 5 but shows the lowest circular polarization. This is opposite to what is expected for IS grains.

2. With the very same passband, two measurements of R Mon made with two different diaphragms show a different sign of circular polarization. This behavior cannot be accounted for by IS grains. We therefore consider the circular polarization to have a circumstellar origin.

b) Failure of Models with Aligned Grains

Following this, the three most likely possibilities for producing the polarization in the "disk" region where the vectors are aligned will be discussed. They are dichroic extinction, single scattering by partially aligned nonspherical dust grains, and multiple scattering in an optically thick disk.

Of course, for the aligned grains to be responsible for the high level of polarization, the alignment efficiency must be high enough, as well as in the proper direction. The direction argument makes the models proposed by Gold (1952) for turbulent gas flow alignment and by Harwit (1970) for grain alignment by transfer of angular momentum from photons both unviable since they yield polarization patterns different from what is observed.

We are then left with magnetic alignment. It has been, up to now, the most widely used mechanism for explaining regions of aligned linear polarization vectors in reflection nebulae. Gething *et al.* (1982), Aspin, McLean, and Coyne (1985) and Warren-Smith, Draper, and Scarrott (1987) proposed this mechanism for R Mon. However, even though the bipolar nebula geometry with a thick equatiorial disk has been recognized for some time for R Mon (Stockton, Chesley, and Chesley 1975; Jones and Dyck 1978; Walsh and Malin 1985) it is not yet clear what is the direction of the magnetic field in the equatorial disk. Scenarios with magnetic fields either parallel (Mestel and Paris 1984; Warren-Smith 1987) or perpendicular (Pudritz and Norman 1983; Uchida and Shibata 1985; Pudritz and Silk 1987) to the equatorial disk have been proposed. In principle, toroidal fields (parallel to the disk) can produce the grain alignment necessary to explain the polarization maps, but not poloidal fields.

Other problems are also present. In the aligned-grain model, preferential extinction by elongated grains is always assumed (Gething *et al.* 1982; Aspin, McLean, and Coyne 1985; Warren-Smith, Draper, and Scarrott 1987). However, the fact that we observe circular polarization implies that the alignment angle of the grains has to rotate somehow across the nebula (Kemp and Wolstencroft 1972; Bandermann and Kemp 1973; Martin 1974). This means a very complex geometry for the magnetic field, but then the linear polarization vectors are no longer aligned. Furthermore, the large optical depth implied by the large amount of extinction needed to explain the high linear polarization is such that multiple scattering will occur. The large values of A_v suggested by Cohen and Kuhi (1979), 4.24, and by Cantó *et al.* (1981), ~ 3, point out in this direction.

On the other hand, if scattering on nonspherical aligned grains is invoked to produce the circular polarization, then linear polarization vectors are not aligned anymore; they tend to be more centrosymmetric. Furthermore, the level of linear polarization for R Mon itself can not be explained by such a model unless the direct stellar light is blocked somehow, which implies again that multiple scattering will occur. It is clear that models with aligned grains cannot explain both linear and circular polarization data for this system and we consider now multiple scattering.

c) Multiple Scattering

The discovery by Beckwith *et al.* (1984) of a halo, much bluer than the star, surrounding R Mon indicates that scattering is present. They suggested that the particles responsible for the scattered light are probably smaller than 1 μm. Also the wavelength dependence of linear polarization is not known precisely because of temporal variations (one should not compare data obtained on different nights); however the observations

published so far suggest that it is rather flat. Such a flat $P(\lambda)$ curve usually implies that scattering by relatively large particles, with size $\sim\lambda$, is occurring if the light source is not completely obscured (see, e.g., Ménard and Bastien 1987, 1988, and references therein). However, if the driving source is totally hidden, we cannot reject the hypothesis that Rayleigh scattering is also present as suggested by Jones and Dyck (1978). In this case, the gaseous component of the disk, via the molecules, could also play a role in producing the polarization.

Beckwith *et al.* (1984) also argue that the minimum scattering optical depth in the "halo" around R Mon is 0.11 and could become much larger than unity depending on the extent of the "halo." According to Shawl (1972, 1975), multiple scattering contributes at least 10% of the intensity for optical depth larger than 0.3 Lefèvre (1988) put this limit even lower on the basis of Monte Carlo simulations: for a simulation with a total extinction of 1.1, the effective opacity is only 0.15, and 55% of the scattered photons are scattered more than once (twice: 28%, three times: 14%, ...). Furthermore, Sargent and Beckwith (1987) found that the emission from the concentration of gas associated with R Mon (Beckwith *et al.* 1986) is optically thick in ^{13}CO.

Finally, BM showed recently that multiple scattering of originally unpolarized stellar light around a thick equatorial disk was able to reproduce polarization maps of YSOs. Patterns of aligned polarization vectors arise naturally, as a consequence of multiple scattering and geometry. There is no problem regarding the high polarization observed. Even circular polarization is predicted to be produced, with the characteristic behavior that it changes sign every quadrant in the disk! From all these arguments we conclude that multiple scattering is indeed responsible for both the linear polarization pattern and the circular polarization detected in R Mon.

A comparison of published linear polarization maps with maps produced with the BM model reveal that the best fit is obtained for an inclination angle of $\sim 75°$. This value is compatible with the fact that a good part of the southern outflow is hidden from our view by this inclined disk. The maximum linear polarization in the disk from this model is 32%–36%, and 70%–90% in the lobes. The maximum circular polarization in the disk from the *same* model is 0.59% for grain radii $a = 0.1$ μm, and 0.86% for $a = 0.2$ μm. The maximum circular polarization values occur at position angles at 45° to the outflow axis, which is at a position angle of $\sim 350°$ (Brugel, Mundt, and Bührke 1984), or $\sim 15°$ when determined from the linear polarization pattern near R Mon (Warren-Smith, Draper, and Scarrott 1987). A more realistic model, which takes multiple scattering properly into account, should yield lower polarization values, closer to what is observed.

However, if we can explain the linear polarization pattern easily with the BM model, as well as the magnitude of the circular polarization, we do not detect the predicted typical circular polarization pattern. Two possible explanations are: (1) the photons flight paths considered in the model are too simple, which could mean that there is a strongly irregular structure near the star, and/or (2) our angular resolution is too large when compared with the expected angular extent of the equatorial disk around R Mon (less than 6″; Sargent and Beckwith 1987).

The observations show that R Mon has a positive circular polarization, as detected with the 3.″9 diaphragm. The equatorial disk begins to dominate the picture at an angular scale between 4″ and 8″, as inferred from our measurements of R Mon with these two apertures. These equatorial structures, where multiple scattering dominates, govern the production of polarization close to the star where we see a pattern of aligned linear polarization vectors and clearly detect circular polarization (at positions 3 and 4, and marginally at position 2). Farther away from the star, as the density in the nebula fades out so does multiple scattering. A centrosymmetric linear polarization pattern is then seen, as single scattering progressively takes over, and no circular polarization is detected (null detection at position 1).

At this point we must emphasize once again that, even though we do not detect the typical circular polarization pattern predicted by BM, we clearly detect an effect caused by multiple scattering in the region around R Mon where the density is enhanced when compared to the bipolar lobes.

This region corresponds to a probable optically thick equatorial disk but is somewhat larger than the inferred 6″ upper limit of Sargent and Beckwith (1987) based on Owens Valley Radio interferometer maximum resolution. It is however much smaller than the ^{12}CO counterpart of this equatorial disk (Cantó *et al.* 1981).

In summary, the fact that the detected circular polarization can be explained *only* by multiple scattering in an equatorial disk and that all linear polarization maps can be explained easily by the same model provide direct evidence for the presence of a flattened equatorial structure around R Mon.

We thank an anonymous referee for useful comments. We are grateful to the Natural Sciences and Engineering Research Council (NSERC) of Canada for financial assistance. We thank the director of the Mont Mégantic observatory for granting observing time and acknowledge the support of B. Malenfant and G. Turcotte, members of the technical staff at the observatory. Finally, we thank E. Borra for the use of his polarimeter, built from an NSERC grant.

APPENDIX

In the ideal case where the alignment of the polarizing optics in the polarimeter is perfect, one measurement taken at any orientation of the instrument will yield a good value for V/I, with no contamination from the linear polarization. On the other hand, for a realistic instrument, i.e., with some (small) deviations in the retardances and alignment angles, averaging two measurements taken at perpendicular positions of the instrument with respect the telescope will cancel to all orders in the normalized Stokes parameters the conversion of linear into circular polarization if no flexure problems are present (i.e., if $\delta_1 = \delta_3$, and $\delta_2 = \delta_4$, see below).

We evaluate from the results of explicit Mueller matrix algebra for the polarizing components (given in detail by Nadeau 1987) the importance of the first-order terms when the alignment is not perfect. We note here that even orders (second and fourth) cancel out exactly in all possible cases, and the third-order terms are at least a factor of 50 smaller than those of the first-order.

For incident radiation with Stokes parameters I, Q, U, and V, the measured circular polarization is given by

$$CP = \frac{1}{4}\left[A\left(\frac{V}{I}\right) + B\left(\frac{Q}{I}\right) + C\left(\frac{U}{I}\right) + \text{negligible third-order terms} \right],$$

where

$$A = -\sin 2\rho[\sin \delta_1 + \sin \delta_2 + \sin \delta_3 + \sin \delta_4],$$

$$B = \cos 4\rho\left[\sin^2\left(\frac{\delta_1}{2}\right) - \sin^2\left(\frac{\delta_2}{2}\right) - \sin^2\left(\frac{\delta_3}{2}\right) + \sin^2\left(\frac{\delta_4}{2}\right)\right] + \cos^2\left(\frac{\delta_1}{2}\right) - \cos^2\left(\frac{\delta_2}{2}\right) - \cos^2\left(\frac{\delta_3}{2}\right) + \cos^2\left(\frac{\delta_4}{2}\right),$$

$$C = \sin 4\rho\left[\sin^2\left(\frac{\delta_1}{2}\right) - \sin^2\left(\frac{\delta_2}{2}\right) - \sin^2\left(\frac{\delta_3}{2}\right) + \sin^2\left(\frac{\delta_4}{2}\right)\right].$$

In the above expressions, ρ is the Pockels cell alignment angle, ideally 45°, and the δs are the retardances, ideally 90°, along the fast (δ_1, δ_3) and slow (δ_2, δ_4) axes for both orientations of the instrument. We allow them to be different to take into account possible flexure problems. Ideally, one should have $A = 4$, and $B = C = 0$. If no major flexure problems are present, then $\delta_1 = \delta_3$, and $\delta_2 = \delta_4$, and B and C almost vanish. If a significant flexure in the instrument/telescope is present, one can see from the above expressions that for realistic values of ρ (43°–47°) and the δs (87°–93°), assuming that (Q/I) and (U/I) are both 15%, that the contamination remains generally a factor of 10, or more, smaller than the $A(V/I)$ term.

REFERENCES

Aspin, C., McLean, I. S., and Coyne, G. V. 1985, *Astr. Ap.*, **149**, 158.
Bandermann, L. W., and Kemp, J. C. 1973, *M.N.R.A.S.*, **162**, 367.
Bastien, P. 1988*a*, in *Proc. Vatican Observatory Conf. on Polarized Radiation of Circumstellar Origin*, ed. G. V. Coyne, *et al.* (Vatican: Vatican Press), in press.
———. 1988*b*, in *NATO Advanced Study Institute, Galactic and Extragalactic Star Formation*, ed. R. Pudritz and M. Fich (Dordrecht: Reidel), 303.
Bastien, P., and Ménard, F. 1988, *Ap. J.*, **326**, 334 (BM).
Beckwith, S., Sargent, A. I., Scoville, N. Z., Masson, C. R., Zuckerman, R., and Phillips, T. G. 1986, *Ap. J.*, **309**, 755.
Beckwith, S., Zuckerman, B., Skrutskie, M. F., and Dyck, H. M. 1984, *Ap. J.*, **287**, 793.
Brugel, E. W., Mundt, R., and Bührke, T. 1984, *Ap. J. (Letters)*, **287**, L73.
Cantó, J., Rodríguez, L. F., Barral, J. F., and Carral, P. 1981, *Ap. J.*, **244**, 102.
Cohen, M., and Kuhi, L. V. 1979, *Ap. J. Suppl.*, **41**, 743.
Cohen, M., Harvey, P. M., Schwartz, R. D., and Wilking, B. A. 1984, *Ap. J.*, **278**, 671.
Garrison, L. M., and Anderson, C. M. 1978, *Ap. J.*, **221**, 601.
Gething, M. R., Warren-Smith, R. F., Scarrott, S. M., and Bingham, R. G. 1982, *M.N.R.A.S.*, **198**, 881.
Gold, T. 1952, *M.N.R.A.S.*, **112**, 215.
Hall, R. C. 1964, *Ap. J.*, **139**, 759.
———. 1965, *Pub. A.S.P.*, **77**, 158.
Harwit, M. 1970, *Nature*, **226**, 61.
Jones, J. J., and Dyck, H. M. 1978, *Ap. J.*, **220**, 159.
Kemp, J. C., and Wolstencroft, R. D. 1972, *Ap. J. (Letters)*, **176**, L115.
Lefèvre, J. 1988, in *Proc. Vatican Observatory Conf. on Polarized Radiation of Circumstellar Origin*, ed. G. V. Coyne, *et al.* (Vatican: Vatican Press), in press.
Martin, P. G. 1974, *Ap. J. (Letters)*, **187**, 461.
Ménard, F., and Bastien, P. 1987, in *IAU Symposium 122, Circumstellar Matter*, ed. I. Appenzeller and C. Jordan (Dordrecht: Reidel), p. 133.
———. 1988, in preparation.
Mestel, L., and Paris, R. B. 1984, *Astr. Ap.*, **136**, 98.
Michalsky, J. J., Stokes, R. A., and Ekstrom, P. A. 1976, *Ap. J. (Letters)*, **203**, L43.
Nadeau, R. 1987, M.Sc. thesis, Université de Montréal.
Nadeau, R., and Bastien, P. 1986, *Ap. J. (Letters)*, **307**, L5.
Notni, P. 1983, *Astr. Nach.*, **306**, 265.
Pudritz, R. E., and Norman, C. A. 1983, *Ap. J.*, **274**, 677.
Pudritz, R. E., and Silk, J. 1987, *Ap. J.*, **316**, 213.
Sargent, A. I., and Beckwith, S. 1987, *Ap. J.*, **323**, 294.
Schmidt, G. D., Angel, J. R. P., and Beaver, A. E. 1978, *Ap. J.*, **219**, 477.
Shafter, A., and Jura, M. 1980, *A.J.*, **85**, 1513.
Shawl, S. J. 1972, Ph.D. thesis, University of Texas, Austin.
———. 1975, *A.J.*, **80**, 595.
Stockton, A., Chesley, D., and Chesley, S. 1975, *Ap. J.*, **199**, 406.
Uchida, Y., and Shibata, K. 1985, *Pub. Astr. Soc. Japan*, **37**, 515.
Vrba, F. J., Schmidt, G. D., and Hintzen, P. M. 1979, *Ap. J.*, **227**, 185.
Walker, M. F. 1956, *Ap. J. Suppl.*, **2**, 365.
Walsh, J. R., and Malin, D. F. 1985, *M.N.R.A.S.*, **217**, 31.
Warren-Smith, R. F. 1987, *Quart. J.R.A.S.*, **18**, 298.
Warren-Smith, R. F., Draper, P. W., and Scarrott, S. M. 1987, *Ap. J.*, **315**, 500.
Zellner, B. 1970, *A.J.*, **75**, 182.

PIERRE BASTIEN, FRANÇOIS MÉNARD, and CARMELLE ROBERT: Département de physique, Université de Montréal, B. P. 6128, Succ. A, Montréal, Québec H3C 3J7, Canada